RSC Advances

PAPER

View Article Online
View Journal | View Issue

Cite this: *RSC Adv.*, 2025, **15**, 2106

Catalytic ozonation of dimethyl phthalate by Ti–MCM-41 in water†

Jishuai Bing,[abcd] Yaoting Wang,[abc] Yiming Zou,[abc] Huimin Zhang,[abc] Zhiling Chou,[abc] Weixiang Cheng[abc] and Xin Xiao *[abd]

Received 6th November 2024
Accepted 7th January 2025

DOI: 10.1039/d4ra07901a

rsc.li/rsc-advances

A Ti–MCM-41 mesoporous molecular sieve catalyst was prepared by a hydrothermal method. Nitrogen adsorption desorption, XRD, TEM and SEM characterization results showed that the catalyst had a large specific surface area, a regular hexagonal pore structure, and titanium doping was uniformly dispersed in MCM-41 molecular sieves. The amount of titanium doping, reaction temperature, and the initial solution pH had important effects on the catalytic ozonation of dimethyl phthalate (DMP) by Ti–MCM-41. In comparison to ozonation alone and MCM-41/O_3, Ti–MCM-41/O_3 exhibited the most effective degradation and mineralization of DMP, with a Si/Ti ratio of 80, a reaction temperature of 25 °C, and an initial solution pH of 5.4. Ozonation alone, MCM-41/O_3, and Ti–MCM-41/O_3 removed 94%, 96%, and 100% of DMP after 15 min of reaction. At 60 min of reaction, the TOC removal rate of the Ti–MCM-41/O_3 process reached 36%, which was 2.4 times that of the O_3 process and 1.9 times that of the MCM-41/O_3 process. The experimental results of initial solution pH and hydroxyl radical capture showed that Ti–MCM-41 had the highest catalytic activity near the zero-charge point, and hydroxyl radicals were active oxygen species. Ti–MCM-41 catalytic ozonation of DMP had synergistic effects and is a promising environmental catalytic material.

1 Introduction

Dimethyl phthalate (DMP) is a kind of refractory phthalate pollutant, which can be detected in different environments such as surface water, groundwater and soil, and has been listed as a priority control pollutant by the United States Environmental Protection Agency (USEPA) and the Ministry of Ecological Environment of China.[1–4] Traditional biological water treatment methods have struggled to degrade and mineralize DMP.[5] Ozone-based advanced oxidation processes (AOPs), including combining ozone with H_2O_2, UV radiation, metallic ions or heterogeneous catalysts, have been widely studied.[6] Heterogeneous catalytic ozonation is a promising technique for removing refractory organic pollutants under mild conditions. It is only necessary to add an appropriate amount of catalyst into the ozonation process, which can not only reduce the amount of ozone, but also speed up the chemical reaction rate and oxidize the byproducts of the ozonation process. The ozonation of organic pollutants has been catalyzed by a variety of catalysts and various methods, but the development of effective and promising catalysts remains crucial.[7–10]

MCM-41 are mesoporous molecular sieves, which could be used as a catalyst, adsorbent, or catalyst carrier due to their large specific surface area and pore volume, uniform and adjustable mesoporous pore size and adsorption capacity. Due to the lack of catalytic ozonation activity of hydroxyl groups on the surface of MCM-41, researchers began to modify MCM-41. The commonly used modification methods include doping method, loading method and grafting method.[11–13] MCM-41 mesoporous molecular sieves were applied in the catalytic field, mainly used in the chemical industry; however, there was limited research on the use of MCM-41 mesoporous molecular sieves and modified catalysts with active components embedded in its framework in the field of environmental catalysis, especially in the treatment of refractory organic pollutants in water by catalytic ozonation.

It had been reported that the Lewis acid site on the catalyst surface could promote the effective decomposition of ozone into active oxygen species, thereby facilitating the mineralization of organic matter.[14–16] TiO_2 was a stable and non-toxic semiconductor photocatalyst, as well as a strong Lewis solid acid catalyst.[17] In the present study, a Ti–MCM-41 mesoporous molecular sieve catalyst was prepared for catalytic ozonation of dimethyl phthalate in water. During the synthesis process of Ti–MCM-41, the acidity of the catalyst can be effectively controlled

[a]*Jiangsu Key Laboratory of Marine Biological Resources and Environment, Jiangsu Ocean University, Lianyungang 222005, China. E-mail: xiaoxin@njust.edu.cn*
[b]*Co-innovation Center of Jiangsu Marine Bio-Industry Technology, Jiangsu Ocean University, Lianyungang 222005, China*
[c]*Lianyungang Environmental Science and Technology Service Center, Lianyungang 222005, China*
[d]*Jiangsu Institute of Marine Resources Development, Lianyungang 222005, China*

† Electronic supplementary information (ESI) available. See DOI: https://doi.org/10.1039/d4ra07901a

by controlling the doping amount of titanium, resulting in the preparation of efficient ozonation catalysts. In this paper, XRD, TEM, SEM and nitrogen adsorption desorption experiments were used to study the structural characteristics of the catalyst. The effects of titanium doping amount, reaction temperature and initial solution pH on DMP catalyzed by Ti–MCM-41 were investigated. The mechanism of catalytic ozonation by Ti–MCM-41 was studied for free radical trapping experiments.

2 Experimental

2.1 Chemicals and reagents

Dimethyl phthalate (DMP) was purchased from Tianjin Kemio Chemical Reagent Co., Ltd. Ultra-pure water was generated using the Milli-Q ultra-pure water analyzer and utilized for solution preparation. Sodium silicate ($Na_2SiO_3 \cdot 9H_2O$), hexadecyltrimethylammonium bromide (CTAB), *tert* butanol (TBA), methanol (CH_3OH), concentrated sulfuric acid (H_2SO_4), hydrochloric acid (HCl), sodium hydroxide (NaOH), and titanium trichloride ($TiCl_3$) were purchased from China National Pharmaceutical Group Chemical Reagent Beijing Co., Ltd. All chemical reagents were analytical pure. The pH of the solution was adjusted with a solution of 2 mol L^{-1} hydrochloric acid and sodium hydroxide.

2.2 Preparation of MCM-41 and Ti–MCM-41

Mesoporous molecular sieves MCM-41 and Ti–MCM-41 were synthesized under alkaline conditions using CTAB as a template and $Na_2SiO_3 \cdot 9H_2O$ as a silicon source.[18] In the preparation process of Ti–MCM-41 (Si/Ti = 80), $NaSiO_3 \cdot 9H_2O$ (28.42 g) was dissolved in 70 mL deionized water stirring at 35 °C. Subsequently, 0.19 g of $TiCl_3$, which was dissolved in 15 mL deionized water, was added to the above mixture and stirred for 15 min. The pH of the mixture was adjusted to 11 by using H_2SO_4 (2 mol L^{-1}) to form a gel. After stirring for 30 min, 7.28 g CTAB dissolved in 25 mL water, was added to the gel and stirred for 30 min. Then the gel was transferred to a Teflon-lined steel autoclave and heated to 145 °C for 48 h. After natural cooling, the product obtained was filtered, washed three times with ultrapure water and dried at 80 °C for 12 h. The obtained sample was calcined at 550 °C for 6 h to remove the template. MCM-41 was prepared by the above procedure in the absence of $TiCl_3$.

2.3 Characterization of catalysts

The crystal form and phase of the catalyst were analyzed on a Scintag-XDS-2000 X-ray diffractometer (XRD) with Cu Kα radiation (λ = 1.540598 Å). The morphology and particle size distribution of the catalyst were analyzed by JEOL 2010 field emission transmission electron microscope (TEM). A Zeiss Ultra 55 scanning electron microscope (SEM) was used to analyze the morphology of catalysts and the acceleration voltage was 10 kV. The specific surface area and porosity of the catalyst were measured using the ASAP-2020 specific surface area meter from Micromeritics in the United States. Porosity was obtained from nitrogen adsorption desorption isotherm and Barrett–Joyner–Halenda (BJH) method. The zero charge point (pH_{pzc}) on the catalyst surface was measured using a Marvin Nano-ZS90 Zeta potentiometer. Specific method: weigh 0.1 g KNO_3 and 0.1 g catalyst into a 1 L volumetric flask to constant volume, shake well, and ultrasonic for 30 min. Measure 60 mL of the above solution and add it to a 100 mL conical flask. Adjust the pH of the solution between 1 and 12 using 0.1 mol L^{-1} HCl or 0.1 mol L^{-1} NaOH; measure the zeta potential value corresponding to each pH value. Each point was measured 3 times and the balance time was 10 seconds. Plot the relationship curve between zeta potential and pH value; and use the interpolation method to obtain the pH when the zeta potential was equal to zero, which was the surface zero charge point of the catalyst.

2.4 Experimental procedures

The catalytic ozonation experiment was conducted in a 1.2 L bubble glass reactor. Using high-purity oxygen as the gas source, O_3 gas was generated through discharge from a 3S-A5 ozone generator (Beijing Tonglin Technology Co., Ltd). After being metered by a flow meter, O_3 gas was dissolved in water with sufficiently small bubbles through a microporous sand core cloth at the bottom of the glass reactor. After stirring with a magnetic stirrer, O_3 can be evenly distributed in the water. In a typical procedure, 1 L dimethyl phthalate around 10 mg L^{-1} aqueous solution and 1 g of catalyst powder were mixed in the reactor under continuously magnetically stir. Gaseous O_3 (10 mg L^{-1}) was continuously bubbled into the reactor through the porous plate of the reactor bottom at a 200 mL min^{-1} flow rate. The residual ozone in the off-gas was trapped by a $Na_2S_2O_3$ solution. Water samples were taken at regular intervals. A 0.1 mol L^{-1} $Na_2S_2O_3$ solution was used to quench the continuous ozonation reaction in the new withdrawn water samples and then water samples were filtered by a 0.45 μm Millipore filter to analyze DMP and total organic carbon (TOC) concentrations. The same procedures were carried out for the control experiments of ozone alone and sorption without ozone. The experimental conditions for catalyst stability were consistent with the above operating methods. The catalyst after use was recycled, dried, and reused. All catalysts activity evaluation data were repeated three times with an experimental error of less than 3%.

2.5 Analytical procedures

The pH of water sample was measured by PHS-3B pH meter, and the electrode model used was E-201-C. The concentration of dimethyl phthalate was determined by a high-performance liquid chromatograph with UV detector (SPD-10AV), with experimental parameters of C18 column (150 mm × 4.6 mm), mobile phase $V_{methanol} : V_{water} = 7 : 3$, flow rate 1.0 mL min^{-1}, DMP detection wavelength 254 nm. TOC analysis was determined by Shimadzu TOC-V_{CPH} total organic carbon analyzer. The concentration of metal ions in solution was analyzed by inductively coupled plasma atomic emission spectrometry (ICP-OES). The gas phase ozone concentration was measured using the IDEAL-2000 ozone concentration detector. The

concentration of dissolved ozone in water was determined using the indigo method.[19]

3 Results and discussion

3.1 Characterization of catalysts

Fig. 1 showed the small angle (1°–8°) and wide angle (10°–90°) XRD images of different samples. In the low angle range (Fig. 1a), it could be seen that the sample exhibits a strong diffraction peaks at 2.2° (100) and two weaker diffraction peaks at 3.8° (110) and 4.4° (200), indicating that the Ti–MCM-41 molecular sieve maintains the ordered mesoporous structure of pure silicon MCM-41 molecular sieve; however, the intensity of the diffraction peak decreased, indicating that titanium doping into the MCM-41 framework resulted in a decrease in the ordering of the material. The wide-angle XRD of Ti–MCM-41 molecular sieve was similar to that of MCM-41 molecular sieve (Fig. 1b), and there was no characteristic crystal phase of TiO_2, indicating that titanium doping was uniformly dispersed in MCM-41 molecular sieve.[20,21]

Fig. 2 showed TEM photos of MCM-41 and Ti–MCM-41 molecular sieves. It could be seen that all samples had one-dimensional long range ordered hexagonal pore structure, which was conducive to organic molecules approaching the active site on the catalyst surface. In addition, no titanium oxide particles were found on the surface of Ti–MCM-41 molecular sieve, indicating that titanium has been uniformly dispersed in the framework of MCM-41 molecular sieve.[22]

The SEM micrographs of MCM-41 and Ti–MCM-41 were shown in Fig. 3. It could be clearly seen that the particles of both MCM-41 and Ti–MCM-41 samples exhibited long-range ordered rod-like structure and the small particles were SiO_2, which did not crystallize well. As shown in Fig. 3b, the bulk titanium oxides could not be observed on MCM-41 surface. It was further verified that titanium oxide doping into the MCM-41 skeleton.

Fig. 4a showed the N_2 adsorption desorption isotherm of MCM-41 and Ti–MCM-41. It could be seen that both MCM-41 and Ti–MCM-41 samples present the type IV adsorption desorption isotherm in the IUPAC classification, indicating that they both had mesoporous structures. In the low partial pressure range ($p/p_0 < 0.2$), due to the monolayer adsorption of N_2 on the pore surface, the adsorption amount of N_2 increases linearly with the increase of p/p_0. At $0.2 < p/p_0 < 0.4$, there was a significant jump in the curve, with a sudden increase in N_2 adsorption capacity and a small hysteresis loop due to the capillary condensation of N_2 in the pore channel, indicating that the

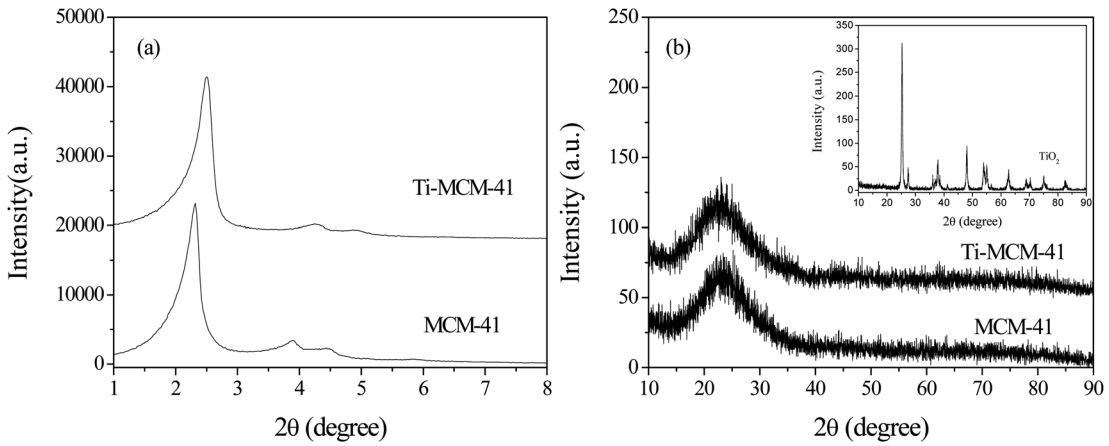

Fig. 1 Low angle (a) and wide-angle (b) XRD patterns of different catalyst samples.

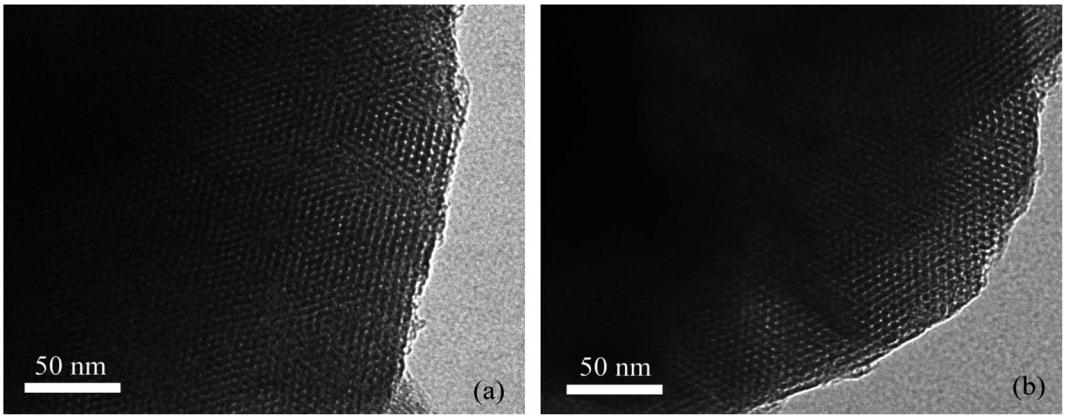

Fig. 2 TEM images of MCM-41 (a) and Ti–MCM-41 (b) catalysts.

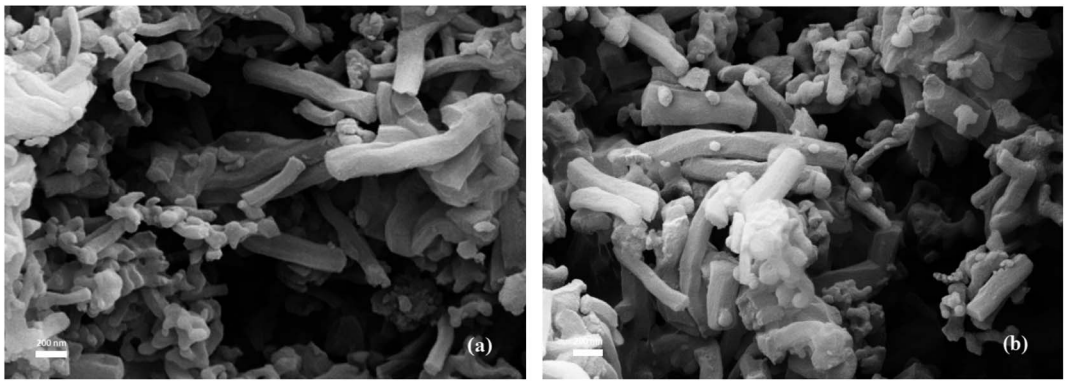

Fig. 3 SEM images of MCM-41 (a) and Ti–MCM-41 (b).

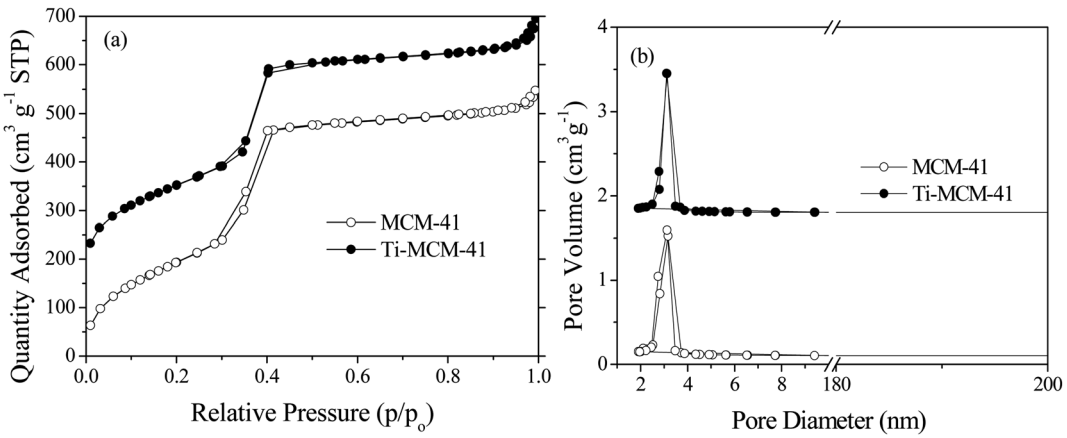

Fig. 4 The N_2 adsorption–desorption isotherms (a) and pore size distribution curves (b) of different catalysts.

sample was within the mesoporous range. When the p/p_0 further increased, N_2 molecules adsorb on the outer surface in monolayer to multilayer, and the adsorption amount tends to flatten out.[23] Fig. 4b showed the pore size distribution of MCM-41 and Ti–MCM-41. The pore size distribution of the sample was relatively narrow, indicating that the sample has a regular mesoporous structure. The specific surface area of the sample was calculated using the BET model, and the pore size and volume were calculated using the BJH model based on the adsorption curve. From Table 1, it could be seen that the specific surface area, pore size, and pore volume of MCM-41 were 1065 $m^2\ g^{-1}$, 3.59 nm, and 0.96 $cm^3\ g^{-1}$, respectively. When Si/Ti was 80, the specific surface area, pore size, and pore volume of Ti–MCM-41 were 920 $m^2\ g^{-1}$, 3.69 nm, and 0.85 $cm^3\ g^{-1}$, respectively. It could be seen that after doping titanium, the specific surface area and pore volume of the catalyst decrease, while the pore size increases. This was because the size of titanium atoms was larger than that of silicon atoms, the doping of titanium into the framework of MCM-41 molecular sieve caused an increase in cell parameters. Similar phenomena also occur when other metal doping entered the framework of MCM-41 molecular sieve.[24,25]

3.2 Effect of titanium content on Ti–MCM-41 catalytic activity

This article investigates the effect of titanium doping on the catalytic ozonation of DMP by Ti–MCM-41, as shown in Fig. 5. It could be seen that titanium doping was beneficial for the removal of DMP and TOC, and the removal rate of DMP and TOC showed a trend of first increasing and then decreasing with the increase of titanium doping amount, reaching the optimal

Table 1 Pore diameter, pore volume, surface area and pH_{pzc} of MCM-41 and Ti–MCM-41

Catalyst	S_{BET} ($m^2\ g^{-1}$)	Pore diameter (nm)	Pore volume ($cm^3\ g^{-1}$)	pH_{pzc}
MCM-41	1065	3.59	0.96	2.28
Ti–MCM-41 (Si/Ti = 80)	920	3.69	0.85	5.4

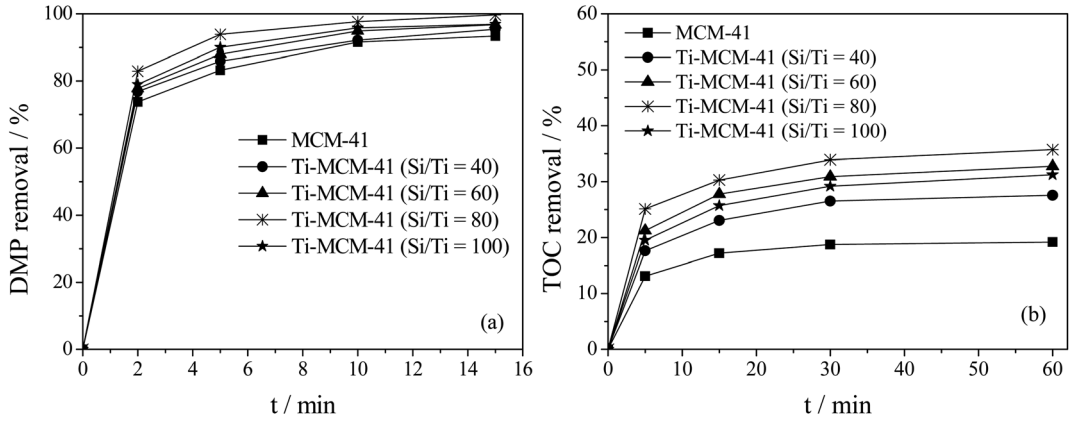

Fig. 5 Effect of titanium doping amount on DMP (a) and TOC (b) removal (initial pH = 5.4, initial DMP concentration = 10 mg L^{-1}, catalyst concentration = 1 g L^{-1}).

value when Si/Ti was 80. As shown in Fig. 5a, after 15 minutes of reaction, the removal rate of DMP by MCM-41/O_3 process was 93.3%; when Si/Ti was 40, Ti–MCM-41/O_3 process was 97%; while Si/Ti was 80, Ti–MCM-41/O_3 process reaches 100%. The amount of titanium doping had a significant impact on the mineralization of DMP (Fig. 5b). After 60 minutes of reaction, the removal rate of TOC by MCM-41/O_3 process was 19%. When Si/Ti was 40, Ti–MCM-41/O_3 process was 28%, while when Si/Ti was 80, Ti–MCM-41/O_3 process reached 36%, significantly improving the mineralization degree of DMP. In the catalytic ozonation reaction system, the active metal sites on the surface of Ti–MCM-41 could promote the decomposition reaction of ozone molecules and generate active oxygen species (such as hydroxyl radical) with stronger oxidation capacity, thus enhancing the oxidation capacity of the system and improving the removal efficiency of pollutants.[26,27] The increase of titanium doping also increased the active site on the surface of the catalyst, so as to increase the yield of active oxygen in the process of Ti–MCM-41 catalytic ozonation of DMP, thus improving the removal rate of DMP and TOC, and reaching the best when Si/Ti was 80. However, excessive titanium doping will reduced the specific surface area of the catalyst, thereby reducing the production of reactive oxygen species and leading to a decrease in DMP and TOC removal rates. Therefore, in the Ti–MCM-41/O_3 system, a Si/Ti of 80 was the optimal Ti doping amount and would be used in subsequent experiments.

3.3 Effect of reaction temperature on catalytic ozonation of DMP

The Ti–MCM-41/O_3 system belong to the three-phase system of gas, liquid, and solid, and the reaction temperature had a significant impact on the system. This article compared the effect of four reaction temperatures (5 °C, 15 °C, 25 °C and 35 °C) on the removal of DMP and TOC in the Ti–MCM-41/O_3 system. The results were shown in Fig. 6. The reaction temperature had a very significant impact on the removal rate of DMP and TOC. When the temperature increased from 5 °C to 25 °C, the removal rates of DMP and TOC significantly increased with the increase of temperature. As shown in Fig. 6a, after 15 min of reaction, the removal rate of DMP was only 87.1% at 5 °C and 93.0% at 15 °C, while it was completely removed at 25 °C; as shown in Fig. 6b, after 60 min of reaction, the TOC removal rate was 23% at 5 °C, 26% at 15 °C, and reached 36% at 25 °C. The influence of temperature on the ozone oxidation reaction

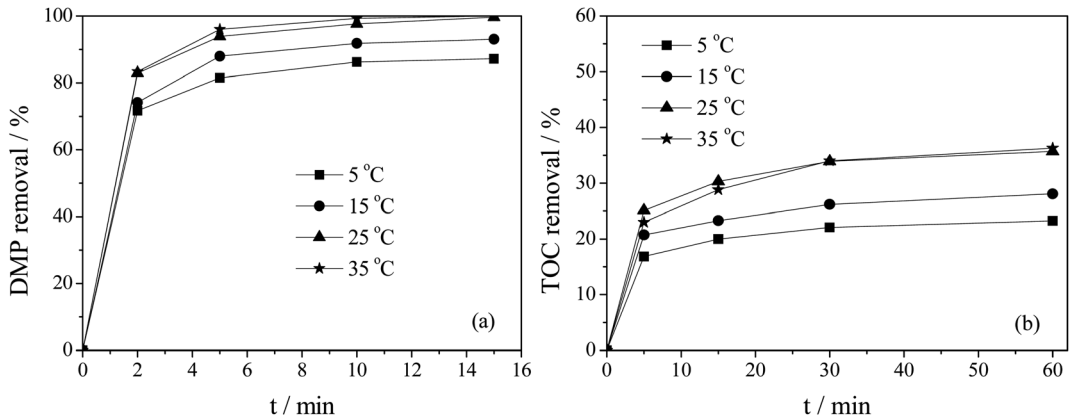

Fig. 6 Effect of reaction temperature on DMP (a) and TOC (b) removal (initial pH = 5.4, initial DMP concentration = 10 mg L^{-1}, catalyst concentration = 1 g L^{-1}, Si/Ti = 80 Ti–MCM-41).

system was mainly manifested in two aspects: on one hand, increasing temperature was beneficial for reducing the activation energy of catalytic reactions, thereby increasing the chemical reaction rate; on the other hand, increasing temperature leads to a decrease in the solubility of ozone in water.[28] From Fig. 6, it could be observed that as the reaction temperature increased to 35 °C, the removal rates of DMP and TOC hardly increased. This was due to the decrease in the solubility of ozone in water and the acceleration of its decomposition rate caused by high temperature. Therefore, 25 °C was chosen as the optimal reaction temperature.

3.4 Comparison of DMP and TOC removal among different processes

As shown in Fig. 7a, when the adsorption reaches equilibrium, the adsorption removal rates of MCM-41 and Ti–MCM-41 for DMP were 8% and 5%, respectively. At 15 min of reaction, the DMP removal rate of ozonation alone was 94%; the MCM-41/O_3 process was 96%, while Ti–MCM-41/O_3 process completely removes DMP. As shown in Fig. 7b, the removal rate of TOC by the single ozonation process was only 15% for 60 min of reaction, indicating that the single ozonation process had limited effect on DMP mineralization. The oxidation of organic matter by ozone could be divided into direct reaction and indirect reaction. The direct reaction was selective. For substances containing unsaturated bonds such as C=C, C=C–O–R, C=C–X, and aromatic compounds containing groups such as –COOH, –NO_2, ozone had a high oxidation capacity.[29] Therefore, ozonation alone could achieve a high DMP removal within 15 min. For some small molecules, such as formic acid and acetic acid produced by ozonation of aromatic compounds, the oxidation rates of ozone to them were only 5.0 and $<4.0 \times 10^{-2}$ L mol^{-1} s^{-1}, respectively, and the ozonation process alone could only mineralize a very small fraction of these compounds.[30] The indirect reaction of ozone was through the self-decomposition reaction induced by ozone in aqueous solution to generate strong oxidant, such as hydroxyl radical, and then oxidize organic matter.[31,32] As shown in Fig. 7b, the TOC removal rate of MCM-41/O_3 process was 19%, mainly due to the adsorption of MCM-41. The TOC removal rate of Ti–MCM-41/O_3 process reached 36%, which was 2.4 times that of O_3 process and 1.9 times that of MCM-41/O_3 process. This was because Ti–MCM-41 promoted the decomposition of ozone molecules to produce strong oxidants, thereby improving the mineralization capacity of the system. Combined with the ozonation alone and the adsorption of Ti–MCM-41, it showed that Ti–MCM-41 and ozone had synergistic effect in the mineralization of DMP.

Fig. 8 showed the activity and stability experiment of Ti–MCM-41 catalyst. After reusing the catalyst 6 times, the removal rates of DMP and TOC only decreased by 5%, and no dissolution of titanium was detected during the reuse experiments. This indicates that the Ti–MCM-41 catalyst had good stability. Ti–MCM-41 was a promising catalytic material for water treatment.

3.5 Discussion on the mechanism

3.5.1 Effect of initial pH on DMP degradation. This article investigated the effect of initial solution pH on Ti–MCM-41 catalytic ozonation of DMP, and the results were shown in Fig. 9. At 60 min of reaction, the TOC removal rates achieved from low to high pH were 20%, 36%, 24%, and 29%, respectively. It could be seen that TOC reaches the highest removal rate at a pH of 5.4. The pH of the solution had a certain impact on the degradation of ozone, thereby affecting the generation of reactive oxygen species. From Table 1, it can be seen that the zero electrical point of MCM-41 was 2.28, while the zero electrical point of Ti–MCM-41 was 5.4, indicating that there were more basic groups on the surface of Ti–MCM-41 catalyst. When initial pH was 5.4, the surface of Ti–MCM-41 was almost neutral. The neutral surface hydroxyl species was the most active in catalyzing ozone decomposition to produce active oxygen species. Since the protonation weakens the nucleophile O of surface hydroxyl groups, the low solution pH would consequently decrease the interaction of the surface hydroxyl groups with ozone. At the high pH, most of the electrophilic H of surface hydroxyl groups gets released into the solution to reduce the chances of the surface Ti–O–H–O_3 interaction, which consequently leads to the low activity of the Ti–MCM-41 in catalyzing active oxygen species generation. From Fig. 9, it could

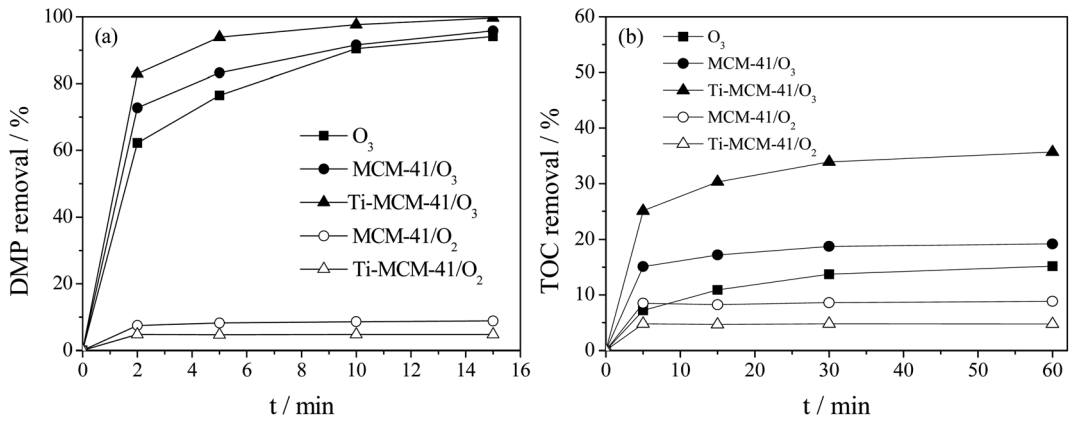

Fig. 7 Comparison of DMP (a) and TOC (b) removal among different processes (initial pH = 5.4, initial DMP concentration = 10 mg L^{-1}, catalyst concentration (if use) = 1 g L^{-1}, Si/Ti = 80 Ti–MCM-41 (if use)).

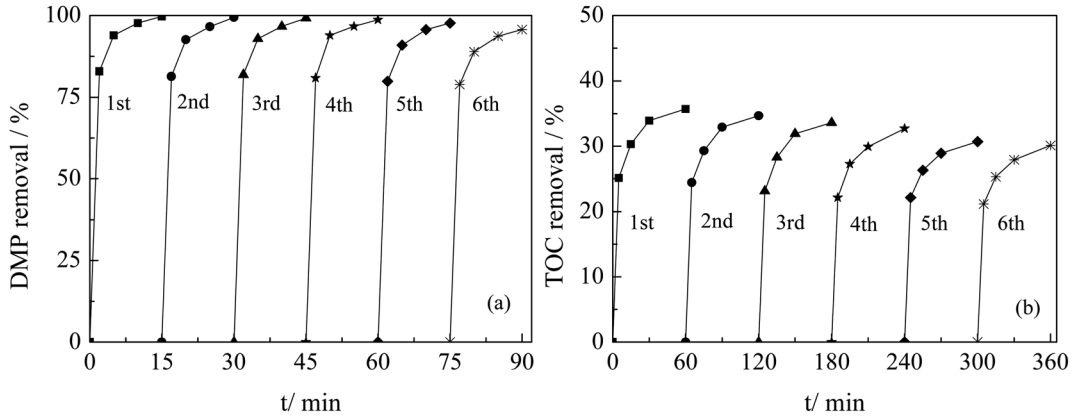

Fig. 8 Activity and stability of Ti–MCM-41 catalyst for ozonation of DMP (a) and TOC (b) (initial pH = 5.4, initial DMP concentration = 10 mg L^{-1}, catalyst concentration = 1 g L^{-1}).

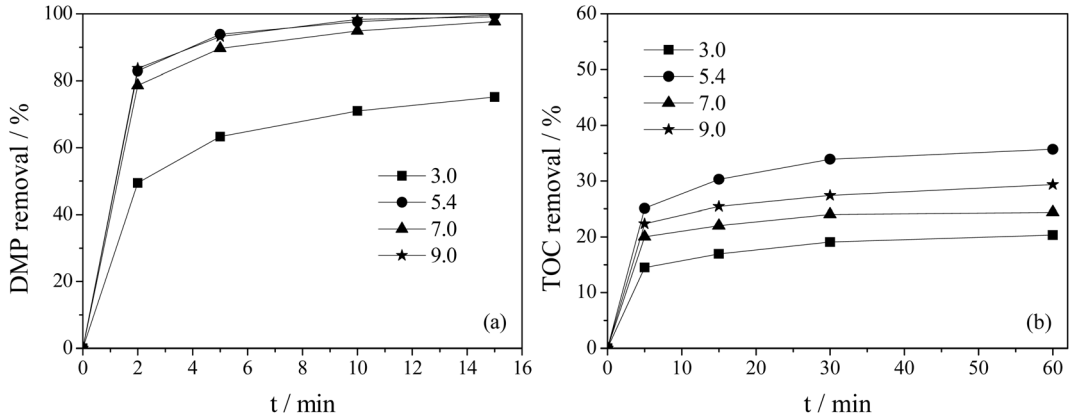

Fig. 9 Effect of initial pH of the solution on DMP (a) and TOC (b) removal (initial DMP concentration = 10 mg L^{-1}, catalyst concentration = 1 g L^{-1}, Si/Ti = 80 Ti–MCM-41).

be seen that the removal rates of DMP and TOC were higher at pH = 9 than at pH = 7, this was because under strong alkaline conditions, ozone could be directly decomposed into hydroxyl radicals, which was conducive to the removal of DMP and TOC in solution.[33,34] In addition, from the perspective of catalyst and organic acid adsorption, although pH < 5.4 was conducive to organic acid adsorption, over-acid conditions would lead to the dissolution of active components; when pH > 5.4, due to electronuclear repulsion, it was not conducive to the adsorption of organic acids. Therefore, at pH 5.4, Ti–MCM-41 showed the highest catalytic activity for ozonation of DMP.

3.5.2 Effect of hydroxyl radical scavenger. *Tert* butyl alcohol (TBA) was a typical free radical inhibitor, and its reaction constant with hydroxyl radical was 6.0×10^8 L mol^{-1} s^{-1}, while the reaction constant with ozone was only 3.0×10^{-3} L mol^{-1} s^{-1}.[35] Therefore, TBA was used to verify whether the Ti–MCM-41 catalytic ozonation of DMP followed the hydroxyl radical mechanism. The experiment investigated the effect of TBA concentrations of 5 mg L^{-1} and 10 mg L^{-1} on Ti–MCM-41 catalytic ozonation of DMP, as shown in Fig. 10. The presence of TBA in the system inhibited the degradation of DMP. At 15 min of reaction, TBA with concentrations of 5 mg L^{-1} and 10 mg L^{-1} reduced the DMP removal rate from 100% to 77% and 58%, respectively. It can be inferred that hydroxyl radical

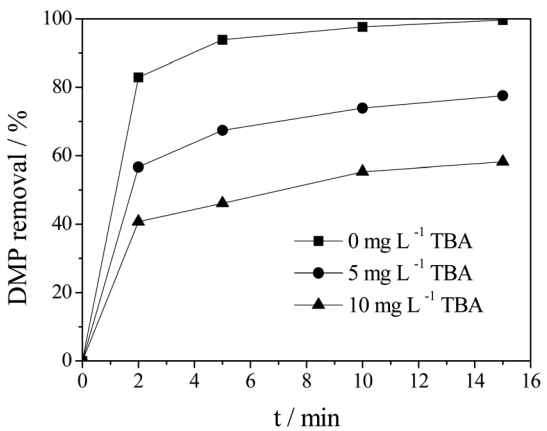

Fig. 10 Influence of TBA in catalytic ozonation of DMP over Ti–MCM-41 (initial pH = 5.4, initial DMP concentration = 10 mg L^{-1}, catalyst concentration = 1 g L^{-1}, Si/Ti = 80 Ti–MCM-41).

oxidation exists in the process of Ti–MCM-41 catalytic ozonation of DMP, and the existence of hydroxyl radical improves the degradation and mineralization of DMP.

4 Conclusion

The Ti–MCM-41 mesoporous molecular sieve synthesized by hydrothermal method was characterized by XRD, TEM, SEM and nitrogen adsorption desorption. The results showed that the catalyst had a large specific surface area and regular hexagonal pore structure, and titanium doping was uniformly dispersed in MCM-41 molecular sieve. The amount of titanium doping, reaction temperature, and initial solution pH had important effects on the activity of Ti–MCM-41 catalyst. When Si/Ti was 80, reaction temperature was 25 °C, and reaction pH was 5.4, the removal rate of DMP and TOC was the best. After 15 minutes of reaction, DMP was completely removed; at 60 minutes of reaction, the TOC removal rate was 36%, while the TOC removal rates of MCM-41/O_3 and ozonation alone were 19% and 15%, respectively. Ti–MCM-41 exhibited the highest catalytic ozonation activity near the zero charge point. Hydroxyl radicals were mainly reactive oxygen species. Ti–MCM-41 had a synergistic effect in the process of catalytic ozonation of DMP and was a promising environmental catalytic material.

Data availability

The data supporting the findings of this study are available within the article.

Conflicts of interest

There are no conflicts to declare.

Acknowledgements

The authors are grateful for the Jiangsu Postdoctoral Fund Project (Contract No. ZKK201904).

References

1 J. Wu, J.-H. Zhou, D.-F. Liu, J. Wu, R.-L. He, Z.-H. Cheng, H.-H. Li and W.-W. Li, Phthalates Promote Dissemination of Antibiotic Resistance Genes: An Overlooked Environmental Risk, *Environ. Sci. Technol.*, 2023, **57**(17), 6876–6887.

2 N. Domínguez-Morueco, S. González-Alonso and Y. Valcárcel, Phthalate occurrence in rivers and tap water from central Spain, *Sci. Total Environ.*, 2014, **500–501**, 139–146.

3 Y. Zhang, P. Wang, L. Wang, G. Sun, J. Zhao, H. Zhang and N. Du, The influence of facility agriculture production on phthalate esters distribution in black soils of northeast China, *Sci. Total Environ.*, 2015, **506–507**, 118–125.

4 S. Mahire, A. S. Tiwana, A. Khan, P. M. Nalawade, G. Bandekar, N. Trehan, U. Mukkannawar, S. Kaur, V. Pandit and P. N. Kamble, Accumulation and effects of persistent organic pollutants and biogeographical solutions: appraisal of global environment, *Arabian J. Geosci.*, 2023, **16**(10), 570.

5 T. An, Y. Gao, G. Li, P. V. Kamat, J. Peller and M. V. Joyce, Kinetics and Mechanism of ·OH Mediated Degradation of Dimethyl Phthalate in Aqueous Solution: Experimental and Theoretical Studies, *Environ. Sci. Technol.*, 2014, **48**(1), 641–648.

6 B. Kasprzyk-Hordern, M. Ziółek and J. Nawrocki, Catalytic ozonation and methods of enhancing molecular ozone reactions in water treatment, *Appl. Catal., B*, 2003, **46**(4), 639–669.

7 E. Issaka, J. N.-O. Amu-Darko, S. Yakubu, F. O. Fapohunda, N. Ali and M. Bilal, Advanced catalytic ozonation for degradation of pharmaceutical pollutants–a review, *Chemosphere*, 2022, **289**, 133208.

8 Y. Wang and G. Yu, Challenges and pitfalls in the investigation of the catalytic ozonation mechanism: a critical review, *J. Hazard. Mater.*, 2022, **436**, 129157.

9 W. Chen, H. He, J. Liang, X. Wei, X. Li, J. Wang and L. Li, A comprehensive review on metal based active sites and their interaction with O_3 during heterogeneous catalytic ozonation process: types, regulation and authentication, *J. Hazard. Mater.*, 2023, **443**, 130302.

10 P. Chhattise, S. Saleh, V. Pandit, S. Arbuj and V. Chabukswar, ZnO nanostructures: a heterogeneous catalyst for the synthesis of benzoxanthene and pyranopyrazole scaffolds *via* a multi-component reaction strategy, *Mater. Adv.*, 2020, **1**(7), 2339–2345.

11 W. Chen, X. Li, Y. Tang, J. Zhou, D. Wu, Y. Wu and L. Li, Mechanism insight of pollutant degradation and bromate inhibition by Fe-Cu-MCM-41 catalyzed ozonation, *J. Hazard. Mater.*, 2018, **346**, 226–233.

12 X. Li, W. Chen, D. Liu, G. Liao, J. Wang, Y. Tang and L. Li, Enhancing water purification through F and Zn-modified Fe-MCM-41 catalytic ozonation, *J. Hazard. Mater.*, 2023, **460**, 132357.

13 X. Cao, T. Ai, Z. Xu, J. Lu, D. Chen, D. He, J. Liu, R. Tian, Y. Zhao and Y. Luo, Insights into the different catalytic behavior between Ce and Cr modified MCM-41 catalysts: Cr_2S_3 as new active species for CH_3SH decomposition, *Sep. Purif. Technol.*, 2023, **307**, 122742.

14 J. Bing, C. Hu, Y. Nie, M. Yang and J. Qu, Mechanism of Catalytic Ozonation in Fe_2O_3/Al_2O_3@SBA-15 Aqueous Suspension for Destruction of Ibuprofen, *Environ. Sci. Technol.*, 2015, **49**(3), 1690–1697.

15 G. Yu, Y. Wang, H. Cao, H. Zhao and Y. Xie, Reactive Oxygen Species and Catalytic Active Sites in Heterogeneous Catalytic Ozonation for Water Purification, *Environ. Sci. Technol.*, 2020, **54**(10), 5931–5946.

16 S. Pandit, R. Shaikh and V. Pandit, Synthesis of 5-unsubstituted-3, 4-dihydropyridine-2-(1*h*)-ones using nbs as a catalyst under solvent free conditions, *Rasayan J. Chem*, 2009, **2**, 907–911.

17 Y. Zheng, J. Shi, H. Xu, X. Jin, Y. Ou, Y. Wang and C. Li, The bifunctional Lewis acid site improved reactive oxygen species production: a detailed study of surface acid site

modulation of TiO_2 using ethanol and $Br^{-\dagger}$, *Catal. Sci. Technol.*, 2022, **12**(2), 565–571.
18 T. Somanathan, A. Pandurangan and D. Sathiyamoorthy, Catalytic influence of mesoporous Co-MCM-41 molecular sieves for the synthesis of SWNTs *via* CVD method, *J. Mol. Catal. A: Chem.*, 2006, **256**(1), 193–199.
19 H. Bader and J. Hoigné, Determination of ozone in water by the indigo method, *Water Res.*, 1981, **15**(4), 449–456.
20 W. H. Yu, C. H. Zhou, X. S. Xu and Z. H. Ge, Catalytic oxidation of 4-*tert*-butyltoluene over Ti-MCM-41, *Chin. Chem. Lett.*, 2007, **18**(3), 341–344.
21 K. Lin, P. P. Pescarmona, H. Vandepitte, D. Liang, G. Van Tendeloo and P. A. Jacobs, Synthesis and catalytic activity of Ti-MCM-41 nanoparticles with highly active titanium sites, *J. Catal.*, 2008, **254**(1), 64–70.
22 N. Igarashi, K. Hashimoto and T. Tatsumi, Catalytical studies on trimethylsilylated Ti-MCM-41 and Ti-MCM-48 materials, *Microporous Mesoporous Mater.*, 2007, **104**(1), 269–280.
23 W. Zhan, G. Lu, Y. Guo, Y. Guo and Y. Wang, Synthesis of Ln-doped MCM-41 mesoporous materials and their catalytic performance in oxidation of styrene, *J. Rare Earths*, 2008, **26**(1), 59–65.
24 J. Bing, L. Li, B. Lan, G. Liao, J. Zeng, Q. Zhang and X. Li, Synthesis of cerium-doped MCM-41 for ozonation of *p*-chlorobenzoic acid in aqueous solution, *Appl. Catal., B*, 2012, **115–116**, 16–24.
25 R. Tismaneanu, B. Ray, R. Khalfin, R. Semiat and M. S. Eisen, Synthesis, characterization and catalytic activity of actinide Th-MCM-41 and U-MCM-41 hexagonal packed mesoporous molecular sieves, *J. Mol. Catal. A: Chem.*, 2001, **171**(1), 229–241.
26 J. Bing, C. Hu and L. Zhang, Enhanced mineralization of pharmaceuticals by surface oxidation over mesoporous γ-Ti-Al_2O_3 suspension with ozone, *Appl. Catal., B*, 2017, **202**, 118–126.
27 L. Zhao, Z. Sun and J. Ma, Novel Relationship between Hydroxyl Radical Initiation and Surface Group of Ceramic Honeycomb Supported Metals for the Catalytic Ozonation of Nitrobenzene in Aqueous Solution, *Environ. Sci. Technol.*, 2009, **43**(11), 4157–4163.
28 R. Huang, H. Yan, L. Li, D. Deng, Y. Shu and Q. Zhang, Catalytic activity of Fe/SBA-15 for ozonation of dimethyl phthalate in aqueous solution, *Appl. Catal., B*, 2011, **106**(1), 264–271.
29 C.-C. Chang, C.-Y. Chiu, C.-Y. Chang, C.-F. Chang, Y.-H. Chen, D.-R. Ji, Y.-H. Yu and P.-C. Chiang, Combined photolysis and catalytic ozonation of dimethyl phthalate in a high-gravity rotating packed bed, *J. Hazard. Mater.*, 2009, **161**(1), 287–293.
30 L. Li, W. Zhu, L. Chen, P. Zhang and Z. Chen, Photocatalytic ozonation of dibutyl phthalate over TiO_2 film, *J. Photochem. Photobiol., A*, 2005, **175**(2), 172–177.
31 J. Nawrocki, Catalytic ozonation in water: controversies and questions. Discussion paper, *Appl. Catal., B*, 2013, **142–143**, 465–471.
32 L. Li, W. Ye, Q. Zhang, F. Sun, P. Lu and X. Li, Catalytic ozonation of dimethyl phthalate over cerium supported on activated carbon, *J. Hazard. Mater.*, 2009, **170**(1), 411–416.
33 T. Zhang, C. Li, J. Ma, H. Tian and Z. Qiang, Surface hydroxyl groups of synthetic α-FeOOH in promoting OH generation from aqueous ozone: property and activity relationship, *Appl. Catal., B*, 2008, **82**(1), 131–137.
34 J. Ma, M. Sui, T. Zhang and C. Guan, Effect of pH on MnO_x/GAC catalyzed ozonation for degradation of nitrobenzene, *Water Res.*, 2005, **39**(5), 779–786.
35 J. Bing, X. Wang, B. Lan, G. Liao, Q. Zhang and L. Li, Characterization and reactivity of cerium loaded MCM-41 for *p*-chlorobenzoic acid mineralization with ozone, *Sep. Purif. Technol.*, 2013, **118**, 479–486.